Simultaneous Measurement of Water Diffusion, Swelling, and Calcium Carbonate Removal in a Latex Paint Using FTIR–ATR

C. M. BALIK* and J. R. XU†

Department of Materials Science and Engineering, Box 7907, North Carolina State University, Raleigh, North Carolina 27695-7907

SYNOPSIS

An *in-situ* FTIR–ATR method has been used to monitor the sorption processes of water and pH 1.3-sulfurous acid in two latex paints and the base polymer common to both. The sorption kinetics could not be described by a simple Fickian model. The spectra also showed evidence of polymer swelling, which was confirmed in separate swelling measurements. Anomalous behavior was noted for the latex paint containing $CaCO_3$ when exposed to sulfurous acid. The amount of water sorbed by this sample went through a maximum, then decreased to a constant level. This was accompanied by similar variations in the degree of swelling of the sample. These changes are explained by the rapid loss of $CaCO_3$ from this particular paint upon exposure to acidic solutions, followed by structural rearrangement to fill in the voids left by the $CaCO_3$ particles. © 1994 John Wiley & Sons, Inc.

INTRODUCTION

Acid rain has been recognized as a potential source of deterioration of paints in recent years.[1] Rain is considered acidic if its pH drops below 5.6, which is the value obtained when water at neutral pH equilibrates with atmospheric carbon dioxide to form small amounts of carbonic acid (H_2CO_3). In previous articles, we reported on the effects of exposure of representative latex and alkyd paint systems to dry SO_2 and its acid formed upon reaction with water (H_2SO_3, sulfurous acid). Solubility and diffusivity measurements have been made for SO_2 in latex and alkyd paints.[2–4] SO_2 has been found to react and cross-link the drying oils in alkyd paints, and the reaction kinetics have been characterized as first order.[4,5] Simple immersion experiments conducted with sulfurous acid and latex paints containing $CaCO_3$ have shown that significant changes occur in the chemical composition of the paint. The $CaCO_3$ is rapidly leached out of the film when immersed in sulfurous acid at pH 2.0, but the removal kinetics slow as pH is increased. The kinetics of the leaching process were characterized as a function of pH using weight loss and attenuated total reflectance Fourier transform infrared spectroscopy (FTIR–ATR) measurements.[6–8] The mechanism for $CaCO_3$ removal appears to be diffusion-controlled at low pH, whereas a chemical reaction between $CaCO_3$ and H^+ ions becomes rate-limiting at higher pH values. The overall weight loss data could still be quantitatively described by an "effective" diffusion coefficient over the entire pH range studied.

The use of FTIR–ATR to measure diffusion of small molecules in polymers is not new. As early as 1975, Lavrentyev et al. suggested its use for measuring diffusivities of solvents and nonsolvents in polymers, to determine independently the diffusion coefficient for different substances in multicomponent media, to appraise the decomposition of adhesive joints under the influence of diffusants, and to observe the various stages of diffusion in multilayer systems.[9] Since then, a number of articles have appeared that use FTIR–ATR to measure small molecule diffusion in polymers[10,11] as well as polymer–polymer interdiffusion.[12,13]

* To whom correspondence should be addressed.

† Current address: Materials Science Institute, Zhongshan University, Guangzhou, People's Republic of China 510275.

Journal of Applied Polymer Science, Vol. 52, 975–983 (1994)
© 1994 John Wiley & Sons, Inc. CCC 0021-8995/94/070975-09

In our previous work, FTIR–ATR measurements of $CaCO_3$ removal were made with free film samples that had been immersed in sulfurous acid for various amounts of time and then removed. These samples therefore contained frozen $CaCO_3$ concentration profiles that varied with immersion time, and numerical methods for extracting a diffusion coefficient from the ATR measurements have been described. Diffusion coefficients measured with the FTIR–ATR method were in excellent agreement with those obtained from weight loss measurements. In this article, we use a real-time FTIR–ATR measurement that provides more insight into structural changes occurring in the paint film during the $CaCO_3$ leaching process. Specifically, it allows us to simultaneously measure three different kinetic events: the diffusion of water into the film, removal of $CaCO_3$ from the film, and swelling of the film.

EXPERIMENTAL

Latex Samples

Three different samples, supplied by Union Carbide Coatings and Emulsions (Cary, NC), were used in this study. Two were fully formulated paints: one containing $CaCO_3$ as an extender and one without $CaCO_3$. The compositions of these paints were given previously.[2] The third sample was the pure latex base polymer, common to both paints, which was a terpolymer of vinyl acetate, vinyl chloride, and butyl acrylate. The T_g of the base polymer was reported as 5°C.

FTIR-ATR Measurements

A CIRCLE (Spectra Tech, Inc.) cylindrical internal reflection accessory was adapted for this study as shown in Figure 1. The paint or polymer sample was cast directly onto the cylindrical ATR crystal using a special device described below. The ends of the coated ATR crystal were sealed in the chamber by two Teflon O-rings that prevented penetration of the diffusant (water and dissolved ions) around the edges of the film. An acid-resistant ATR crystal (AMTIR-1, also from Spectra Tech) having a refractive index of 2.5 was used.

To obtain a uniform film thickness along the ATR crystal, a special casting device was built. It consists of a rotating axis on which the ATR crystal was mounted, a driving motor with variable speed control, and a doctor blade whose angle and distance from the ATR crystal could be adjusted. The thickness of the film was controlled by a micrometer that changed the distance of the doctor blade from the rotating crystal. A film was prepared by simply pouring the latex suspension along the ATR crystal while rotating, with the doctor blade in the desired position. After the film was reasonably dry, the doctor blade was backed away from the crystal and the rotation of the rod was continued for several hours to allow the film to become rigid enough to prevent flow. The coated rod was then placed in a desiccator containing anhydrous $CaSO_4$ for a minimum of 5 days before diffusion measurements were initiated. The films adhered very well to the ATR crystal. The film thicknesses were determined with a sensitive micrometer (MSC Industrial Supply Co.) and ranged from 94 to 152 μm (3.7–6.0 mil).

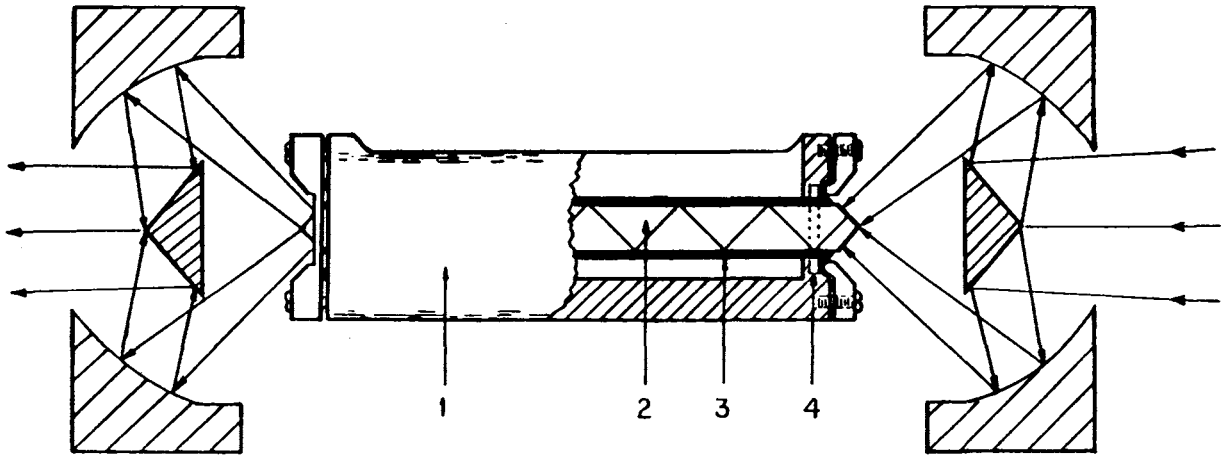

Figure 1 Sampling accessory for making ATR measurements: (1) CIRCLE cell containing liquid diffusant; (2) ATR crystal; (3) polymer sample; (4) Teflon O-rings.

To initiate a diffusion experiment, the penetrant (pure water or sulfurous acid) was poured into the cell, which was then sealed and placed in an Analect FX-6260 FTIR spectrometer equipped with an MCT detector. Spectra were collected as a function of time, and 32 scans were accumulated for each spectrum, which took about 40 s. The sampling time for each spectrum was thus set in the middle of the spectral acquisition period. The spectrometer software was used to perform peak integrations and spectral subtractions.

When latex films containing $CaCO_3$ are immersed in an acidic solution, the pH tends to increase as the $CaCO_3$ is removed from the film and reacts with H^+ ions. To maintain constant pH, either a flow system must be used or a large excess of H^+ ions must be present (i.e., low pH). For the following experiments, we chose the latter route, and used sulfurous acid with a pH of 1.3. Measurements made before and after these experiments showed that the pH of the surrounding solution did not change. This pH is below that for acid rain, which typically has a pH of 3–5.

Optical Microscopy

An Olympus BH reflection optical microscope was used to directly observe and measure the swelling of the latex films upon sorption of water. A cell was designed to simulate the experimental conditions used in the FTIR–ATR method. One side of the latex film was exposed to deionized distilled water, and the thickness of the film was measured as a function of time as the water was absorbed. To create a film cross section without plastically deforming the sample, the following procedure was used: One side of a glass microscope slide was scribed with a glass cutter, and the latex film was cast onto the other side. After the film had dried, the slide was broken under liquid nitrogen, exposing a clean, undeformed cross section of the polymer film.

ATR Principles and Data Analysis

Each time an internal reflection occurs in the ATR crystal, an evanescent wave is set up in the sample, whose electric field amplitude E drops off exponentially with distance from the crystal surface x, i.e.:

$$E = E_0 \exp(-x/d_p) \qquad (1)$$

E_0 is the electric field amplitude at the crystal surface. The region of the sample probed by this evanescent wave is typically characterized by a penetration depth, d_p, given by

$$d_p = \frac{\lambda}{2\pi n_1[\sin^2\theta - (n_2/n_1)^2]^{0.5}} \qquad (2)$$

where λ is the infrared wavelength; n_1 and n_2, the refractive indices of the ATR crystal and sample, respectively, and θ, the angle of incidence of the infrared beam. For most polymers, the penetration depth is typically less than $\lambda/3$.

During the diffusion of a penetrant into a polymer sample, the composition of the region sampled in an ATR experiment changes with time. The contribution to the intensity of a selected penetrant infrared band at time t from penetrant molecules located at distance x from the ATR crystal is proportional to the product of the penetrant concentration, $c(x, t)$, and the evanescent wave electric field amplitude, $E(x)$. The total intensity will be proportional to the integral of this product over the entire film thickness, h, and can be written in the form of a relative intensity ratio:

$$\frac{I(t)}{I(\infty)} = \frac{\int_0^h \frac{c(x,t)}{c_0}\cdot\frac{E(x)}{E_0}\,dx}{\int_0^h \frac{E(x)}{E_0}\,dx} = \frac{A(t) - A(0)}{A(\infty) - A(0)} \qquad (3)$$

Here, c_0 is the (constant) penetrant concentration outside of the polymer sample; $I(t)$, the intensity of the penetrant infrared peak at time t; and $I(\infty)$, the intensity at equilibrium ($t = \infty$), at which point the relative concentration $c(x, t)/c_0 = 1.0$. $I(t)/I(\infty)$ is measured experimentally via the second equality, in which $A(t)$, $A(0)$, and $A(\infty)$ represent the integrated absorbance of the selected penetrant peak at time t, $t = 0$, and at $t = \infty$, respectively. For diffusion of penetrant *out of* the sample, c_0 and $A(0)$ are redefined as the initial (uniform) concentration of penetrant in the sample and the initial integrated absorbance of the selected penetrant infrared peak, respectively.

If the diffusion of the penetrant in the polymer is Fickian, the relative concentration $c(x, t)/c_0$ can be replaced by the appropriate solution to Fick's second law, the integral in the numerator of eq. (3) can be evaluated analytically, and the diffusion coefficient can be extracted from fits of the resulting equation to experimental measurements of $I(t)/I(\infty)$. In a previous article, we used a numerical method to do this[6]; here, we use the analytical so-

lution. For diffusion of a penetrant into both sides of a thin film of thickness $2h$, the relative concentration is[14]:

$$\frac{c(x,t)}{c_0} = 1 - \frac{4}{\pi}\sum_{n=0}^{\infty}\frac{(-1)^n}{2n+1}\cos\frac{(2n+1)\pi x}{2h} \times \exp\left[-\frac{(2n+1)^2\pi^2 Dt}{4h^2}\right] \quad (4)$$

The boundary conditions used to arrive at this solution were

$$c = 0, \quad t = 0, \quad -h < x < h$$
$$c = c_0, \quad t \geq 0, \quad x = \pm h$$

The concentration profiles for this solution are symmetrical about the midplane ($x = 0$) of the film, resulting in a no-flux condition ($dc/dx = 0$) at $x = 0$. The same solution also applies for diffusion into a film of thickness h with an impermeable surface at $x = 0$. This is precisely the situation for the ATR experiment, with the ATR crystal surface at $x = 0$. Inserting eqs. (4) and (1) into eq. (3) and integrating yields the following expression for $I(t)/I(\infty)$:

$$\frac{I(t)}{I(\infty)} = 1 - \frac{8r}{\pi(1-e^{-r})}\sum_{n=0}^{\infty}\frac{\pi e^{-r} + (-1)^n\{2r/(2n+1)\}}{4r^2 + \pi^2(2n+1)^2} \times \exp\left[-\frac{(2n+1)^2\pi^2 Dt}{4h^2}\right] \quad (5)$$

where $r = h/d_p$. For many cases of practical interest, and for the purposes of this article, $r \gg 1$, and eq. (5) simplifies to

$$\frac{I(t)}{I(\infty)} = 1 - \frac{4}{\pi}\sum_{n=0}^{\infty}\frac{(-1)^n}{2n+1}\frac{1}{1+\{(\pi/2r)(2n+1)\}^2} \times \exp\left[-\frac{(2n+1)^2\pi^2 Dt}{4h^2}\right] \quad (6)$$

In practice, nonlinear regression methods are used to fit $I(t)/I(\infty)$ vs. t data to a five-term version of eq. (6), which is adequate to determine D to three significant figures.

We assume that d_p (and therefore r) remains constant in our analysis of diffusion data. Strictly speaking, this is not true since the composition and thus the refractive index of the region sampled by the evanescent wave is changing with time as the penetrant diffuses into the polymer. However, $I(t)/I(\infty)$ as calculated from eq. (4) is very insensitive to variations in r in our range of interest. Plots of $I(t)/I(\infty)$ vs. Dt/h^2 were essentially superimposable for $r \geq 10$. For film thicknesses ≥ 50 μm (2 mil), this covers d_p values that correspond to any wavelength in the midinfrared region. Under these conditions, diffusion coefficients obtained from fits of eq. (6) to experimental data will, for practical purposes, be independent of the choice of infrared wavelength, as well as changes in the sample refractive index.

RESULTS AND DISCUSSION

Latex Polymer Base

Three of the ATR spectra obtained during sorption of deionized distilled water into a 114 μm film of the latex polymer base are displayed in Figure 2 and show increasing amounts of water as measured by the broad OH peak around 3400 cm^{-1}. The relative intensity of this peak is plotted vs. time normalized by the square of film thickness in Figure 3. Scaling the time axis this way is standard for diffusion measurements and permits comparison between data collected for different film thicknesses. The solid line in Figure 3 is an attempt to fit the Fickian model to these data. The fit is not good at medium to long times, indicating that water sorption by this polymer has substantial non-Fickian character. In spite of this, the diffusion coefficient obtained, 6.78×10^{-8} cm^2/s, is not unreasonable for water in this polymer and compares favorably with 4.3×10^{-8} cm^2/s, the value obtained by Kishimoto et al.[15] for water in pure poly(vinyl acetate) at 25°C. Our terpolymer contains about 33 mol % vinyl acetate.

Also plotted in Figure 3 is the relative intensity of the OH peak in a latex base polymer sample exposed to sulfurous acid at pH 1.3. The same general curve shape is seen, but the time to reach an equilibrium value is much longer, and it appears that equilibrium has not been attained in the time scale of the experiment. This data provided a poorer fit to the Fickian model than did the sample exposed to distilled water, yielding $D = 1.62 \times 10^{-8}$ cm^2/s. The simple diffusion model apparently does not describe the sorption of water or sulfurous acid by the latex base polymer, nor was it successful when ap-

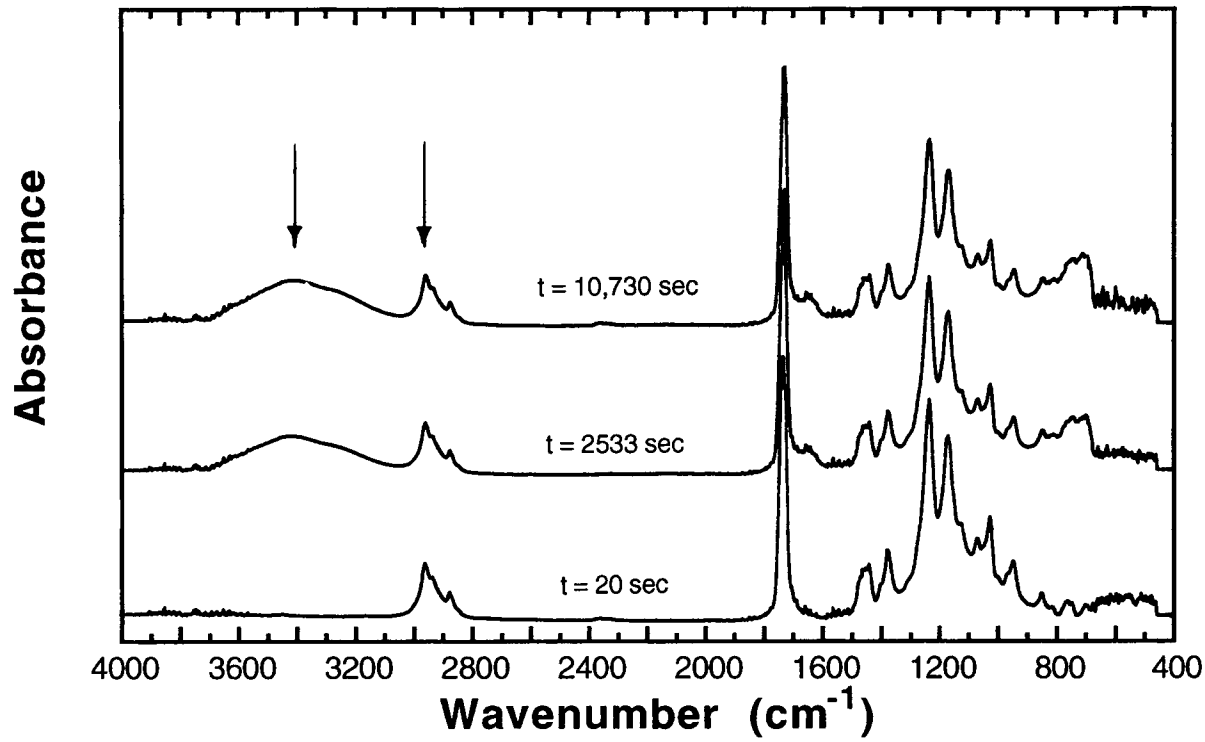

Figure 2 FTIR-ATR spectra obtained at various stages of sorption of distilled water by the latex base polymer (114 μm thick). Variations in the water OH peak at 3400 cm^{-1} and the polymer CH peak at 2950 cm^{-1} (indicated by arrows) were followed with time.

plied to the data for the paint samples formulated from this polymer. Therefore, the kinetic mechanism(s) occurring during water or sulfurous acid sorption cannot be specified from the FTIR-ATR data alone.

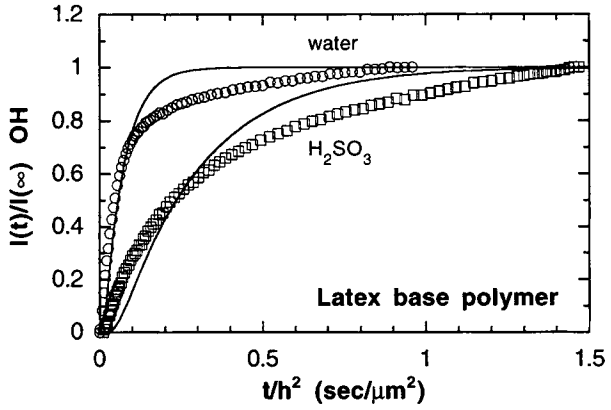

Figure 3 Relative intensity of the water OH peak during sorption of distilled water (circles) and sulfurous acid (squares) by the latex base polymer. The solid lines represent the best fit to the data by the Fickian model. Film thicknesses = 114 μm (water sample) and 152 μm (H_2SO_3 sample).

The non-Fickian aspects of Figure 3 could be attributed to swelling of the polymer and/or loss of contact of the polymer film with the ATR crystal surface as water reaches that interface. Independent measurements have confirmed the occurrence of swelling. Some evidence for swelling or loss of contact can also be found in the FTIR-ATR spectra. As mentioned above, $I(t)/I(\infty)$ is very insensitive to changes in d_p or the refractive index. Changes in this ratio therefore reflect changes in the number (concentration) of infrared-absorbing groups in the region sampled by the evanescent wave. Close examination of the spectra in Figure 2 show that the intensities of the polymer peaks decrease with time as water is absorbed, which is consistent with swelling. This is illustrated for the C—H peak at 2950 cm^{-1} in Figure 4(a). The data in Figure 4(a) are the mirror image of the data for water sorption in Figure 3. A cross plot shows a nearly perfect linear relationship between these two relative intensities, as shown in Figure 4(b). This type of relationship between the OH peak for water sorption and the CH polymer peak was consistently obtained for all samples.

Direct measurement of swelling was made for the latex base polymer using a reflection optical micro-

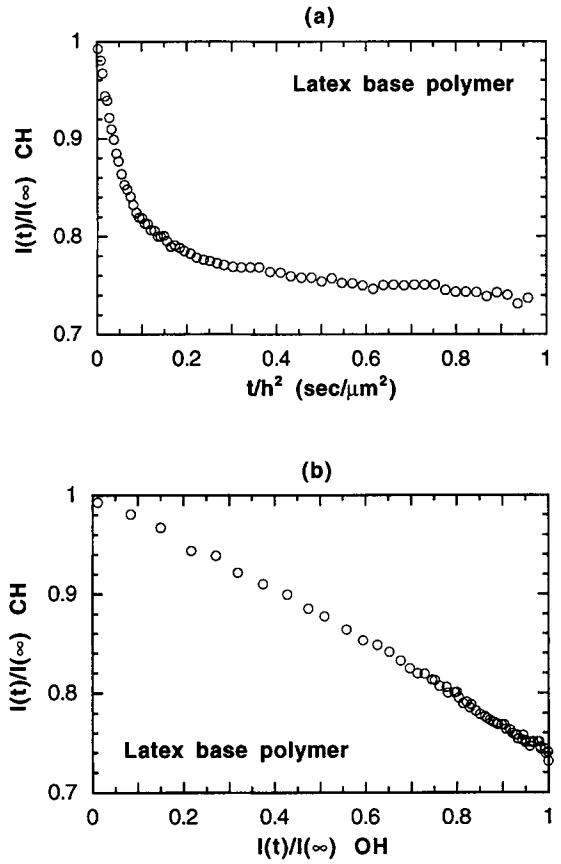

Figure 4 (a) Relative intensity of the polymer CH peak during sorption of distilled water by the latex base polymer. (b) Relationship between the water OH peak and the polymer CH peak during sorption of distilled water by the latex base polymer.

scope. A film (initially 147 μm thick) was cast on glass and exposed to water on one side, simulating the conditions of the FTIR–ATR experiment. The thickness of the film was measured as a function of time as water diffused into the polymer. Results are plotted in Figure 5, showing that the polymer reaches swelling equilibrium at $t/h^2 \approx 0.7$. The FTIR–ATR data for water in Figure 3 are also very close to equilibrium at this point. The relative expansion attained at equilibrium as measured microscopically (about 15%) is less than the FTIR–ATR value based on the intensity loss of the CH peak [about 26%, Fig. 4(a)]. It is tempting to attribute this difference to loss of contact of the polymer film with the ATR crystal; however, we have no further evidence for this. In any case, the optical microscopy confirms that a significant amount of swelling takes place and accounts at least partially for the decreasing intensity of the polymer infrared peaks shown in Figure 2.

Latex Paint Without $CaCO_3$

FTIR–ATR spectra obtained during sulfurous acid sorption by the latex paint formulated without $CaCO_3$ are shown in Figure 6. Comparison with Figure 2 shows additional broad peaks around 800 and 1100 cm^{-1}, which are due to china clay and other inorganic additives. Plots of the OH peak relative intensity for exposure to distilled water and sulfurous acid are shown in Figure 7. The same general trend as in Figure 3 is observed; the sorption of distilled water by the sample reaches equilibrium faster than does sulfurous acid. However, the equilibration time for both water and sulfurous acid is significantly less in this paint sample than in the base polymer. The loss of intensity for the polymer CH peaks (not shown) is equally rapid, and again mirrors the gain in intensity of the OH peaks. Apparently, water saturates the sample/ATR crystal interface faster for the formulated paint than for the base polymer; a somewhat surprising result. A more rapid water uptake would be indicative of a higher effective diffusivity for water in the paint or a more rapid swelling rate for the paint, both being rather unlikely. The formulated paint contains approximately 40% by volume of inorganic fillers (pigment and china clay). The filler would be expected to act as a reinforcing agent, which would hinder swelling and diffusion of small molecules. Indeed, we have shown that the diffusivity of SO_2 gas in this paint is slightly lower than in the base polymer.[2] We were also not able to detect any pinholes or microscopic breaks that would provide fast diffusion paths in the formulated paint films, yet a more rapid uptake of water was consistently observed for samples prepared from both formulated paints as compared to the latex polymer base.

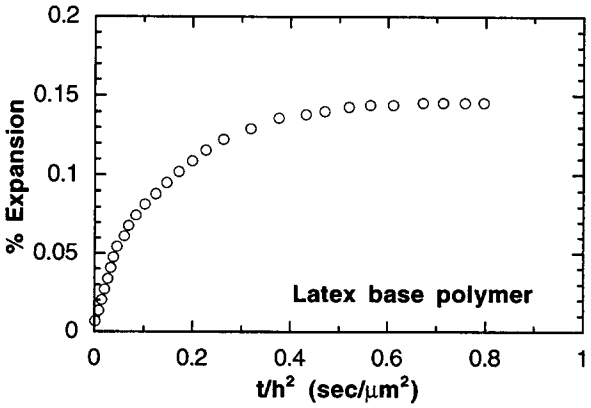

Figure 5 Swelling of the latex base polymer in the thickness direction during sorption of distilled water as measured microscopically. Initial film thickness = 147 μm.

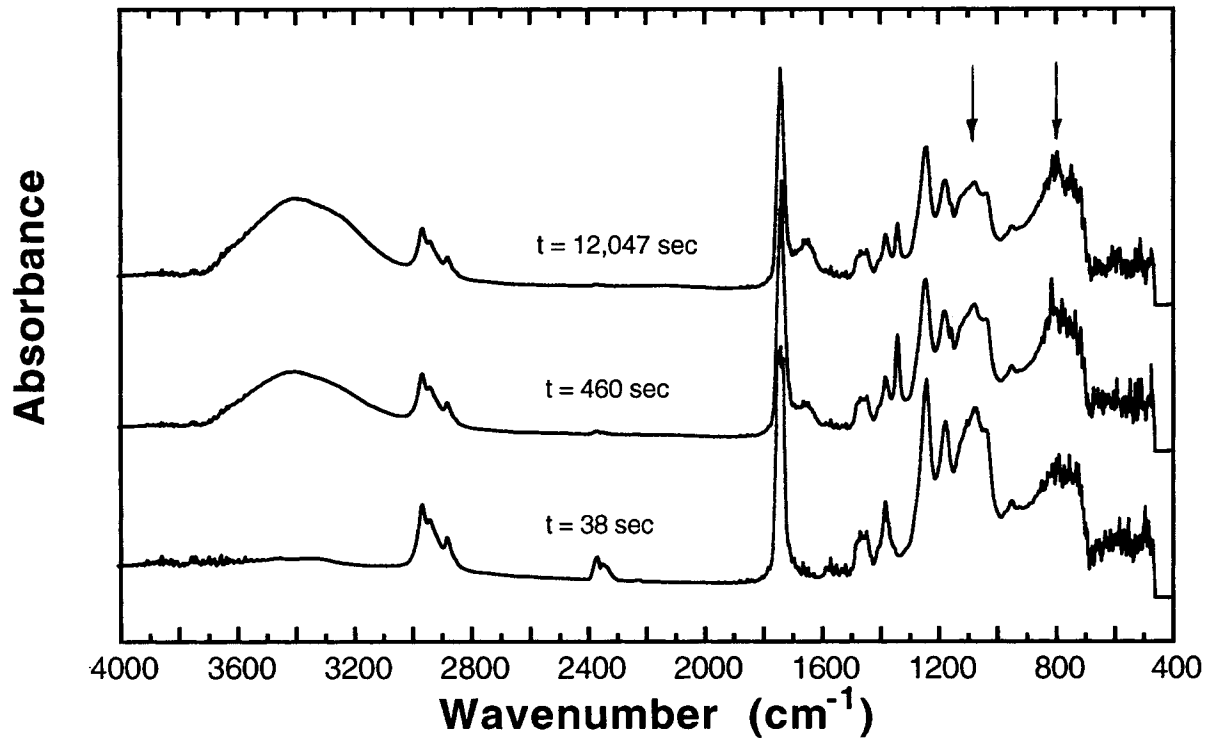

Figure 6 FTIR–ATR spectra obtained at various stages of sorption of sulfurous acid by the latex paint without $CaCO_3$ (94.0 μm thick). Arrows indicate peaks due to inorganic paint additives.

Latex Paint with $CaCO_3$

Exposure of the latex paint containing $CaCO_3$ to distilled water produced essentially the same results as shown in Figure 7 for the paint without $CaCO_3$. Water saturated the ATR crystal/sample interface more rapidly than it did in the latex polymer base.

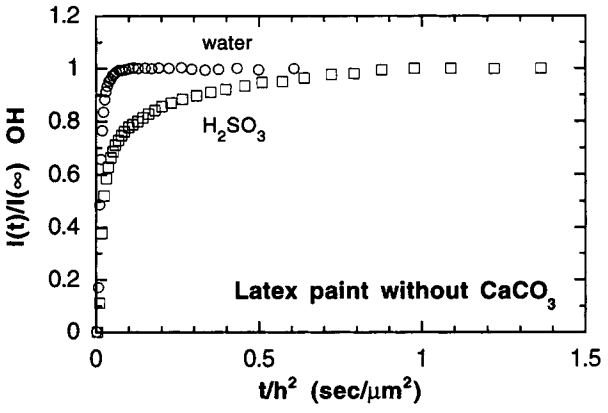

Figure 7 Relative intensity of the water OH peak during sorption of distilled water (circles) and sulfurous acid (squares) by the latex paint without $CaCO_3$. Film thicknesses = 127 μm (water sample) and 94.0 μm (H_2SO_3 sample).

More interesting were the results obtained upon exposure of the $CaCO_3$-containing paint to sulfurous acid: Spectra are shown in Figure 8. Peaks associated with the $-CO_3$ group are evident at 1416 and 875 cm^{-1}. As reported earlier,[7] $CaCO_3$ is rapidly removed upon exposure of this paint to acidic solutions, and these peaks disappear. This is shown by the circles in Figure 9, which represent the relative intensity of the 1416 cm^{-1} $CaCO_3$ peak. This intensity drops rapidly and monotonically to zero. Conversely, the intensity of the OH peak for water sorption by this paint does not increase monotonically to an equilibrium value, as was the case for the other paint and base polymer. Instead, it increases rapidly to a maximum and then decreases more slowly to a final equilibrium value, as shown by the diamonds in Figure 9. The OH intensity variation is again mirrored by the intensity for the polymer CH peak (squares, Fig. 9), which goes through a minimum at the same time the OH peak attains its maximum. Both these extrema occur shortly after the $CaCO_3$ peak reaches zero intensity.

This behavior was unique to the paint containing $CaCO_3$, and we attribute it to the rapid loss of $CaCO_3$ from this sample. This creates voids in place of the $CaCO_3$ particles, which are immediately filled with

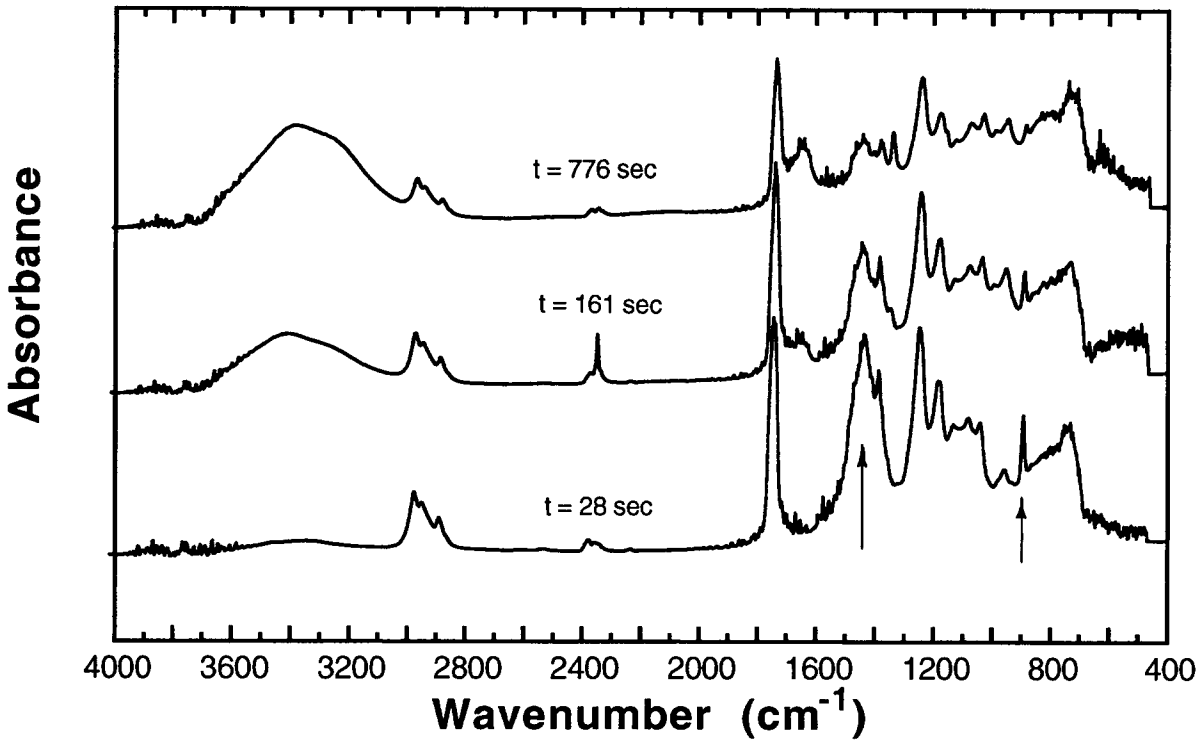

Figure 8 FTIR–ATR spectra obtained at various stages of sorption of sulfurous acid by the latex paint containing $CaCO_3$ (94.0 μm thick). Peaks associated with $CaCO_3$ are evident at 875 and 1416 cm^{-1} (arrows), which rapidly disappear upon exposure to sulfurous acid.

water molecules, causing a rapid increase in OH peak intensity. This is supported by the fact that the OH intensity does not peak until just after the $CaCO_3$ intensity drops to zero. Eventually, the polymer relaxes to fill in the voids, excluding the excess water molecules in the voids, causing a reduction in the OH peak intensity and a corresponding increase in the polymer CH peak intensity. We estimate the amount of deswelling at 14–16%. The volume percent of $CaCO_3$ in this paint is 16%,[2] which agrees well with the difference between the maximum in the OH peak intensity and its final value (15%) and the corresponding difference for the CH peak intensity (14%).

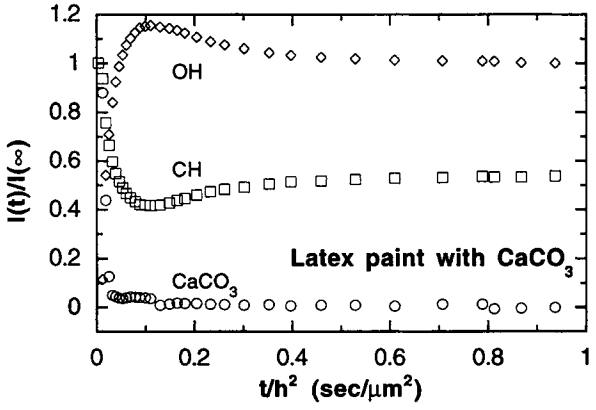

Figure 9 Relative intensities of the water OH peak (diamonds), polymer CH peak (squares), and the $CaCO_3$ peak at 1416 cm^{-1} (circles) during sorption of sulfurous acid by the latex paint containing $CaCO_3$. Film thickness = 94 μm.

Similar maxima in sorption curves have been noted by others for polymers in which some type of structural rearrangement such as crystallization is induced by the sorption process.[16–18] Vrentas et al. also attributed maxima in sorption curves in the ethyl benzene/poly(ethyl methacrylate) system at 120°C (50° above T_g) to structural rearrangements caused by polymer relaxation.[19]

We rule out the possibility that the turnaround in the OH and CH peak intensities is due to loss and reestablishment of sample contact with the ATR crystal. If so, we would have expected to see it at least once during the many experiments carried out with the other samples when exposed to sulfurous acid or to the $CaCO_3$ sample when exposed to water. However, this behavior was noted only for the

$CaCO_3$ sample when it was exposed to sulfurous acid. Second, there is good agreement between the amount of $CaCO_3$ in the sample and the amount of deswelling, as noted above.

CONCLUSIONS

An FTIR–ATR method has been used to follow the diffusion of water and pH 1.3 sulfurous acid into two latex paints and the base polymer common to both. The data could not be described by a simple Fickian model. It was also noted that the polymer peak intensities decreased concurrently and at the same rate as the increase in the water peak intensity in all cases. Independent measurements showed that this is at least partially due to swelling of the polymer by water, although we cannot rule out the possibility that some loss of contact occurs between the sample and the ATR crystal as water reaches that interface, which would also reduce the polymer peak intensities. Either of these anomalies could account for the failure of the Fickian model. All samples equilibrated faster when exposed to distilled water than when they were exposed to sulfurous acid, and the time required for water or sulfurous acid to saturate the ATR crystal/sample interface was much shorter for both formulated paints than for the latex polymer base.

In accordance with previous results, exposure of the $CaCO_3$-containing paint to sulfurous acid resulted in rapid loss of the $CaCO_3$, as revealed by the loss of intensity for the $CaCO_3$ peaks. In this case, the OH peak intensity for water uptake went through a maximum and the polymer peak intensities went through a minimum. These extrema occurred shortly after the $CaCO_3$ peak dropped to zero intensity, suggesting that voids are formed in the sample upon immediate dissolution and removal of the $CaCO_3$ particles, which are then slowly removed as the polymer relaxes and excludes the water molecules residing in the voids. The FTIR–ATR method provides a unique way to follow these kinetic events as they happen.

The authors gratefully acknowledge the U.S. Environmental Protection Agency for support of this work through Cooperative Agreement #CR-814166-01-0.

REFERENCES

1. R. Babobian, Ed., *Materials Degradation Caused by Acid Rain,* ACS Symposium Series 318, American Chemical Society, Washington, DC, 1986.
2. B. J. Hendricks and C. M. Balik, *J. Appl. Polym. Sci.,* **40,** 953 (1990).
3. C. M. Balik, B. J. Hendricks, and W. H. Simendinger, *Proc. ACS Div. Polym. Mater. Sci. Eng.,* **63,** 554 (1990).
4. W. H. Simendinger and C. M. Balik, *J. Coat. Technol.,* **64,** 37 (1992).
5. W. H. Simendinger and C. M. Balik, to appear.
6. J. R. Xu and C. M. Balik, *Appl. Spectrosc.,* **42**(8), 1543 (1988).
7. J. R. Xu and C. M. Balik, *J. Appl. Polym. Sci.,* **38,** 173 (1989).
8. J. R. Xu and C. M. Balik, *J. Appl. Polym. Sci.,* **39,** 1957 (1990).
9. V. V. Lavrentyev, V. Y. Popov, and R. M. Vasenin, *Vysokomol. Soed.,* **A17**(7), 1621 (1975).
10. V. K. Hemmelman and H. Brandt, *Exp. Tech. Phys.,* **37,** 195 (1989).
11. G. T. Fieldson and T. A. Barbari, *Polymer,* **34**(6), 1146 (1993).
12. J. G. Van Alsten and S. R. Lustig, *Macromolecules,* **25,** 5069 (1992).
13. E. Jabbari and N. A. Peppas, *Macromolecules,* **26,** 2175 (1993).
14. J. Crank, *The Mathematics of Diffusion,* 2nd ed., Oxford University Press, New York, 1975.
15. A. Kishimoto, E. Maekawa, and H. Fujita, *Bull. Chem. Soc. Jpn.,* **33,** 988 (1960).
16. N. Overbergh, H. Berghmans, and G. Smets, *Polymer,* **16,** 703 (1975).
17. R. P. Kambour, E. E. Karasz, and J. H. Daane, *J. Polym. Sci. A-2,* **4,** 327 (1966).
18. W. V. Titow, M. Braden, B. R. Currell, and R. J. Loneragan, *J. Appl. Polym. Sci.,* **18,** 867 (1974).
19. J. S. Vrentas, J. L. Duda, and A. C. Hou, *J. Appl. Polym. Sci.,* **29,** 399 (1984).

Received July 29, 1993
Accepted September 23, 1993